Dynamics of the Mount Nyiragongo lava lake

Burgi, Pierre-Yves; Darrah, T. H.; Tedesco, D.; Eymold, W. K.

How to cite

BURGI, Pierre-Yves et al. Dynamics of the Mount Nyiragongo lava lake. In: Journal of biomaterials applications, 2014, vol. 119, n° 5, p. 4106–4122. doi: 10.1002/2013JB010895

This publication URL: https://archive-ouverte.unige.ch/unige:44048

Publication DOI: 10.1002/2013JB010895

Dynamics of the Mount Nyiragongo Lava Lake

P.-Y. Burgi[1,2*], T.H. Darrah[3], D. Tedesco[4,5], and W.K. Eymold[3]

[1] Society of Volcanology Genève, C.P. 75, CH-1261 Le Vaud, Switzerland

[2] IT Department, University of Geneva, 1211 Genève, Switzerland

[3] Divisions of Solid Earth Dynamics and Water, Climate and the Environment, School of Earth Sciences, The Ohio State University, Columbus, OH 43210-1398

[4] DISTABIF, Second University of Naples, 81100 Caserta, Italy

[5] International Organization of Migrants, 1211 Genève, Switzerland

[*]Corresponding Author; e-mail: pierre-yves.burgi@unige.ch

This article has been accepted for publication and undergone full peer review but has not been through the copyediting, typesetting, pagination and proofreading process which may lead to differences between this version and the Version of Record. Please cite this article as doi: 10.1002/2013JB010895

Abstract

The permanent and presently rising lava lake at Mount Nyiragongo constitutes a major potential geological hazard to the inhabitants of the Virunga volcanic region in the Democratic Republic of Congo (DRC) and Rwanda. Based on two field campaigns in June 2010 and 2011, we estimate the lava lake level from the southeastern crater rim (~400 m diameter) and lava lake area (~46,550 m^2), which constrains, respectively, the lava lake volume (~9 x 10^6 m^3) and volume flow rate needed to keep the magma in a molten state (0.6 to 3.5 m^3 s^{-1}). A bi-directional magma flow model, which includes the characterization of the conduit diameter and funnel-shaped lava lake geometry, is developed to constrain the amount of magma intruded/emplaced within the magmatic chamber and rift-related structures that extend between Mt. Nyiragongo's volcanic center and the city of Goma, DRC, since Mt. Nyiragongo's last eruption (January 17, 2002). Besides matching field data of the lava lake level covering the period 1977 to 2002, numerical solutions of the model indicate that by 2022, 20 years after the January 2002 eruption, between 300 to 1700 x 10^6 m^3 (0.3 to 1.7 km^3) of magma could have intruded/emplaced underneath the edifice, and the lava lake volume could exceed 15 x 10^6 m^3.

Keywords

Mount Nyiragongo, Virunga Volcanic Province, lava lake instability, buoyancy force, bi-directional magma flow model, self-regulating magmatic system, intrusive vs. extrusive volcanic activity.

1 Introduction

Mount Nyiragongo, located on the western branch of the East African Rift System (EARS) (Figure 1A), is considered Africa's most active volcano [Tedesco et al., 2007a; d'Oreye et al., 2008]. It is a steep stratovolcano that extends 3,469 m above sea level and contains the world's largest continuously active lava lake within its crater. Within the last four decades, Mt. Nyiragongo's lava lake has twice (1977 and 2002) drained catastrophically through its southern flank [Demant et al., 1994; Komorowski et al., 2002/2003; Tedesco et al., 2007a].

In January 2002, this drainage occurred through a set of conductive and pervasive fissures that visibly opened on the southern flank of the volcano (Figure 2). The 2002 eruption released voluminous lava flows (Figure 1B) that flowed through the city of Goma to Lake Kivu. This eruption devastated approximately 15% of the city, including part of the international airport, killed ~200 people, and displaced at least 250,000 additional residents [Baxter et al., 2002/2003; Tedesco et al., 2007b]. A future eruption similar to that in 2002 would pose a substantial threat to the health and social stability of this fragile geopolitical location.

While the assessment of all regional geological hazards remains a challenge (e.g., Tassi et al.; 2009; Cuoco et al.; 2013), we have developed a mathematical model for the long-term evolution (over 40 years) of the lava lake. This model, which considers the geometry of the lava lake and the buoyancy-driven bi-directional magma flow, provides insight into the mechanisms that control the volume of magma presently in place versus the magmatic material that enters the volcanic edifice and is stored below. We use this model to differentiate these processes as a way to address the potential hazards associated with future eruptions. We also apply Witham and Llewellin's [2006] generic lava lake system model to account for observed instabilities of the lava lake-conduit system occurring on a shorter time scale (from a few hours to several days).

2 Volcanic Setting

Complete reviews of the tectonic, geologic, and volcanic setting of Mount Nyiragongo are available elsewhere in the literature (White and McKenzie, 1989; Nyblade et al., 2000; Ebinger, 2005; Sebai et al., 2006; Tedesco et al., 2007a; Tedesco et al., 2010; Smets et al., 2014). Here, we include a concise description of only parameters relevant to lava lake dynamics and our model.

Since its “European” discovery in 1894 [Tazieff, 1984], Mt. Nyiragongo's steep-walled, 1200 m-wide summit crater has contained a semi-permanent but highly fluctuating lava lake that has experienced several overflows and major eruptions. Rising lava lake levels, along with seismic/tectonic events, likely triggered the N-S trending lateral 1977 and fissural 2002 eruptions that extend between Mt. Nyiragongo and the City of Goma [Carn, 2002/2003; Komorowski et al., 2002/2003; Poland, 2006; Tedesco et al., 2007a; d'Oreye et al., 2011]. The sequential increase in lava lake volume and rapid fissural eruptions are likely responsible for Mt. Nyiragongo's peculiar crater morphology [Tazieff, 1984; Durieux, 2002/2003] that includes three distinct volcanic platforms (P1 (prior to 1977), P2 (1995-2002), and P3 (2003-present)) (Figure 3A). The sustained magma filling through the plumbing system (Figure 2) and active convection continues within this lava lake through the present [Durieux, 2002/2003; Platz et al., 2004; Tedesco et al., 2007a; Smithsonian Institution/USGS Weekly Report 2011-2013], which resulted in the formation of “Platform 3” (P3).

3 Observations and Methods

Our team conducted two field expeditions from June 14 to 24, 2010 and May 30 to June 9, 2011 to the vigorously active Mt. Nyiragongo volcano. During these field campaigns, a comprehensive series of field observations included monitoring the lava lake level, documenting the physical configuration and rate of activity at the lava lake, and topographic measurements.

3.1 Telemetry

The lava lake dimensions and surface level were measured by infrared laser rangefinder with embedded tiltmeter to correct for elevation angle (TruPulse 200 device Laser Technology Inc.). While previous reports used the lava lake diameter to characterize its size, we provide the length of the main E-W and N-S axes because of its marked elliptical shape and then calculate an average diameter for convenience. The N-S axis used direct telemetric measurements of the northern and southern rims, although lava lake infrared radiation required the need for longer measurement times. Because of the complex topography on P2, we relied on triangulation methods using two P2 observation points to determine the E-W axis; these points were situated on the E-W axis and separated by a distance of 100 m to improve accuracy (< 1 m).

Darkly colored (black) rocks reduced infrared laser beam reflection and limited the application of this measurement method on the lava lake. Fortunately, sustained periods of low lava lake activity produced white deposits on top of the floating slabs, allowing for efficient laser reflection. However, these light colored (nearly white) areas were ephemeral and did not exist for sufficient periods of time during periods of intense lava lake activity. Under these conditions, the rangefinder accuracy was ~30 cm and ~1 m for white and darker floating slab targets, respectively. Because of the variable reflection between different color lava surfaces, we apply the lowest error bounds to all calculations reported herein.

3.2 Lava Lake Activity

Mt. Nyiragongo has a long established reputation as an intensely active lava lake with rapid lake level fluctuations and lava overflows. These phenomena were first reported at Mt. Nyiragongo by Le Guern [1987], documented throughout the period from 2003 to 2009 [Tedesco et al., 2010], and also observed during both the 2010 and 2011 field campaigns. Activity included cycles of strong lava fountaining, continuous release of large gas plumes (predominantly H_2O, CO_2, and SO_2 [Sawyer et al., 2008]), and rapid and chaotic movement of partially cooled plates of fresh lava that either move to the lava lake margin or are re-consumed with the lava lake by internal lava lake activity.

In June 2010, we performed near continuous visual observations from 7 am to 10 pm for 10 successive days with more sporadic observations at night. In addition, photos and videos of the lava lake were taken from P2. Throughout most of the period of observation, the lava lake surface remained within a few meters below the top of the levee (Figures 3B). However, for three consecutive days (from June 19-21), we witnessed lava overflowing the levee and flooding P3, situated 15 m below the top of the levee.

Overflowing was the result of a slow rise of the lava lake level, which started early in the afternoon, with the largest overflows occurring at the end of each day (Table 1). Small overflows were the result of active lava fountains occurring next to the lake border concomitant to the rise of the lava lake level reaching the top of the levee (but not overreaching it). In this case flooding was of limited span, of short duration (less than 10 minutes), and generally stopped on the crater floor (P3) at the foot of the levee (Figure 4A). Large overflows occurred whenever the lava lake level overreached the top of the levee and produced major floods lasting between 15 to 45 minutes, covering P3 with several hundreds of square meters of fresh lava (Figure 4B). All overflows occurred on the East and Northeast sides of the lava lake, corresponding to the direction where lava fountains collide into the

levee along the border of the lava lake.

The following field season (June 2011), during which we also cumulated 10 observation days, the lava lake level was stable at about -12 m (±1m) from the levee from May 30 until June 3. During this time, we did not observe any overflows (Figure 5A) until the late afternoon of June 3 when we witnessed a major drainage (Figure 5B), concomitant with a large burst within the lava lake; this drainage dropped the lava lake level by ~25 m in less than one minute. In the hours following this drainage event, the convective motion of the lava lake stopped and was followed by a period of strong Strombolian activity in the northern part of the lava lake that reached heights of ~50 m with metric-size bubbles.

The lava lake level continued to drop stepwise by increments of ~2 m during the next three days (from June 4 to the morning of June 6), with a total drop (including the first major pulse) of ~33 m, placing the lava lake surface to almost 45 m below the levee on P3 (Figure 5C).

4 Results

4.1 Lava Lake Level and Depth

Accurately determining the lava lake level is critical to determining the risks associated with any prospective Mt. Nyiragongo eruptions. Past activities have shown rapid ascents of the lava lake level, followed by slower ascents (e.g., between 1953 and 1965), with quiescent periods during which no lava lake activity was visible and the crust eventually solidified (e.g., 1965-1966, 1983-1994, and 1995-2001) [Tazieff, 1984; Le Guern, 1987; Durieux, 2002/2003]. Such quiescent time periods have been followed by periods of recrudescence in the activity that led to lava fountaining and rapid ascent of the lava lake level (e.g., between 1970 and 1972, and between 1994 and 1995 [GVN, 1995; Durieux, 2002/2003]).

Prior to the 1977 and 2002 eruptions, the lava lake surface was ~155 m and ~250 m below the SE crater rim, respectively [Durieux, 2002/2003] (Figures 6A and 6B, Table 2). Subsequent to the 1977 and 2002 eruptions, the lowermost level of the newly shaped crater, whose parameters are essential to estimate the depth of the lava lake, has been estimated to between 800 m [Durieux, 2002/2003] and 900 m [Tedesco et al., 2007a] below the SE crater rim, respectively.

Following the January 2002 drainage, the lava lake level has risen consistently [Durieux, 2002/2003; Tedesco et al., 2007a; Durieux, 2008; and present study] (Figure 6C and Table 3). In June 2010, the altitude of P3 was estimated at 3,025 m (Figure 2), with the lava lake surface ~15 m above it (i.e., the lava lake was ~385 m below the SE crater rim). In early June 2011, the elevation of P3 had not significantly changed, but the lava lake level was about 15 m below P3 (i.e., the lava lake was ~415 m below the SE crater rim). Lava lake depth is thus estimated at ~500 m at this time.

4.2 Crater Morphology and Lava Lake Size

The June 2010 field measurements indicate an elliptic lava lake shape 230 m and 220 m wide for the E-W and N-S axes, respectively (surface of 40,000 m^2). Those dimensions expanded respectively to 260 m and 228 m within a year (measured in June 2011), with an equivalent area of ~46,550 m^2 (average diameter 244 m).

The field measurements of the lava lake diameter performed since 1982 (Tables 2 and 3) show a positive correlation with lava lake depth, appropriately modeled with an inverted cone characterized by an averaged slope (repose angle) and width of the flat bottom (Figure 2). Using linear regression based on the least square method applied to the 1982-2001 and 2002-2011 compiled data, one respectively gets 54.5 and 79° for the repose angle (γ in Figure 2), and 118 m and 46 m for the width of the flat bottom (Figure 7).

4.3 Conduit Diameter

To our knowledge there is no estimation in the literature for Mt. Nyiragongo's conduit diameter, contrary, for instance, to Mt. Erebus, where it has been suggested to range from 4 to 10 m [Calkins et al., 2008; Zandomeneghi et al., 2013]. However, on June 3, 2011 (at around 08:00 pm) we witnessed a remarkable 25 m drop in the lava lake level in less than one minute (a time lag representing an upper bound given a gas plume temporarily hindered visibility of the lava lake), which involved a magma volume estimated at ~1.0 x 10^6 m^3. From these results we observe that (1) the conduit length has only a minor effect on the maximum volume flow rate (and thus on time length) and (2) a conduit diameter of 15 m is the most consistent with our observations (draining of the lava lake in less than one minute). Thus, in the rest of this paper, we set d_c to 15 m (See Appendix A for calculations).

4.4 Effective Radiation Temperature and Energy Flux

The lava lake surface thermal fluxes (comprising radiative and convective components) are highly sensitive to the effective radiation temperature (T_e). The estimation of T_e is dependent on the proportion of the lava lake surface occupied by the crust (f_{crust}), the exposed molten material (f_{lava}) mainly consisting of active lava fountains, and the cracks (f_{crack}), the latter of which are composed of a red, glowing central core surrounded by a cooler crust (Figure 3A) [Burgi et al., 2002]. With the proportion values given in Appendix A, we obtain T_e = 828 K. This value is smaller than field estimates of T_e =948 K based on lava lake activity in 1959 [Le Guern, 1987] and larger than the 2005-2006 estimates of T_e =650 K from satellite (MODIS) remote sensing data of the Mt. Nyiragongo radiant flux [Wright and Pilger, 2008]. However, our value is within the range of 803 to 835 K reported by Spampinato et al. [2013] based on ground-based thermal imagery recorded for the first half of 2012. Taking T_{air} = 15.5 °C (average field value measured on platform P3 in June 2011), the convective cooling component is calculated to be ~350 MW. Thus, the total heat loss ($\Phi_{tot} = \Phi_r + \Phi_{conv}$) for the June 2011 lava lake is estimated to ~1.5 GW (see Appendix A for calculations).

4.5 Mass Flux

The sustained presence of an actively convecting lava lake requires exceptional geodynamic conditions [Tazieff, 1994; Harris et al., 1999; Oppenheimer et al., 2009]. In most volcanic systems, the exsolution of magmatic volatiles and the cooling of lava at ambient atmospheric temperatures are sufficient to reduce the system's entropy and lead to rapid lava quenching or crystallization [Francis et al., 1993]. Because Mt. Nyiragongo contains the largest continuously active lava lake in the world, it is an optimal location to explore these phenomena.

There are two main end-member enthalpy models, one corresponding to dyke intrusion and the other to cumulate emplacement [Francis et al., 1993; Harris et al., 1999]. Mt. Nyiragongo is located in an extensional environment likely to promote rifting and dyking. Based on data from the January 2002 eruptive event, d'Oreye et al. [2008] and Wauthier et al. [2012] used InSAR analysis to infer the presence of two dyke intrusions. One formed as a shallow dyke at ~2000 m depth on average and associated with a 20 km-long eruptive fissure, while the second was 6000 m deep and extended to ~40 km. Both dyke

intrusions were emplaced along fissures situated ~3000 m below the city of Goma. Thus, we hypothesize that at least part of magma could be emplaced in these dyke intrusions.

Dyke intrusions in these conditions correspond to enthalpy model parameters of Δf = 0.25 and ΔT_{magma} = 50 °C [Francis et al., 1993], which yields q = 9230 kg s^{-1}, or equivalently, 0.2 kg s^{-1} m^{-2} (Table 4; See Appendix A for calculations). These values are similar to those reported for the year 1972 [Harris et al., 1999]. Assuming a degassed magma density of 2650 kg m^{-3} (corresponding to nephelinite density, Carn, 2002/2003), q corresponds to a volume flow rate $Q_{mo} = q / \rho_d$, that is, 3.48 m^3 s^{-1} (See Appendix A for calculations). Alternatively, applying the cumulate emplacement enthalpy model wherein Δf = 1 and ΔT_{magma} = 400 °C [Francis et al., 1993], we get q =1704 kg s^{-1} and Q_{mo} = 0.64 m^3 s^{-1} (Table 4; See Appendix A for calculations). These two models provide end-member estimates. Thus, we consider that during the simultaneous operation of dyke intrusion and cumulate emplacement and/or reservoir mixing, the Q_{mo} ranges between 0.6 to 3.5 m^3 s^{-1}.

5 The Model

Complex interactions between magma density and lithospheric subsidence rates control the ratio of intrusive to extrusive volcanic activity. In the case of Mt. Nyiragongo, the lava lake level provides a proxy for extrusive magma flow, although past eruptions have shown that only a fraction of magma erupts. Reasonable estimates of the volume of magma contained within the lava lake can be made accurately through field measurements.

Conversely, estimating the intruded/emplaced volumes beneath Mt. Nyiragongo requires numerical modeling. We develop a model for emplacement volumes by considering a bi-directional magma flow in a constrained system composed of the magmatic chamber (whose geometry is unknown) and the lava lake (whose geometry is calculated assuming an inverted cone, Figure 2) connected through a vertical conduit, which we take as cylindrical. To conform our model to field data, we consider the time evolution of the lava lake level from June 1982 to June 2011 (spanning nearly 30 years, Figures 6B and 6C), during which data on the lava lake level evolution has been reported with sufficient sampling rates.

To express the evolution of the lava lake volume (V_l) and the volume of intruded/emplaced magma (V_{in}), we consider two volume flow equations,

$$\frac{dV_l}{dt} = Q(t) - Q_{mo}(t) \qquad (1)$$

$$\frac{dV_{in}}{dt} = Q_{mo}(t) \qquad (2)$$

where the ascending volume flow rate at any time *t* is denoted by $Q(t)$, and the volume flow rate needed to keep the lava lake in a molten state, $Q_{mo}(t)$, is proportional to the lava lake surface $A_l(t)$:

$$Q_{mo}(t) = \alpha_{mo} A_l(t) \qquad (3)$$

$Q_{mo}(t)$ provides a measure of the cooler, more degassed, and denser magma volume circulation flow with respect to depth, which we relate to a single parameter, α_{mo}, dependent on the chosen enthalpy model (Table 4). This parameter plays an important role in the model as it determines (through Equations (1) to (3)) the intrusive-extrusive magma ratio. We constrain its value to remain within the range of volume flow rates estimated in Section 4.5.

The downward volumetric flux of the denser degassed magma must be matched by an equal or higher (for the lava lake to grow) upward flux of less dense magma from the magmatic chamber. A buoyancy-driven pressure can account for such a bi-directional flow. The magnitude of the involved (over)-pressure is calculated by applying Archimedes' principle, which assumes the mass of the fluid displaced ($\Delta\rho V_{in}$), times gravity acceleration (*g*), divided by the (ascending) conduit area. We take the density difference $\Delta\rho$ between degassed (descending) and gas-rich (ascending) magma to range from 70 to 120 kg m^{-3} [Witter et al., 2004; Huppert and Hallworth, 2007].

For a laminar flow (which applies given the ascending magma speed is typically < 0.1 m s^{-1}), the ascending volume flow rate in a vertical circular conduit follows Poiseuille's law [e.g., Bansal, 2010],

$$Q(t) = \frac{(P_c(t) - \rho_a g h_l(t) - \rho_a g h_c)\pi d_a^4}{128 \mu h_c} \qquad (4)$$

whereby $P_c(t)$ is the pressure at the base of the conduit, $h_l(t)$ is lava lake depth, h_c is conduit length, and d_a and ρ_a are the ascending conduit diameter and the density of gas-rich ascending magma, respectively, with $\rho_a = \rho_d - \Delta\rho$. For d_a, we account for the fact that the rising magma occupies a fraction of the conduit with the other part being occupied by descending magma. Consistent with previous experimental values [Stevenson and Blake, 1998], we set d_a to represent 60% of the total conduit diameter, d_c.

Because of the inverted cone shape of the lava lake, whenever the lava lake volume (V_l) increases due to the influx of fresh magma, both the lava lake surface $A_l(t)$ and lava lake depth $h_l(t)$ increase. Based on Equation (4), we see that $Q(t)$ must remain positive to ensure continuous upward flow, while any $h_l(t)$ increases will require that $P_c(t)$ increases proportionally. Furthermore, to compensate for the increase of $Q_{mo}(t)$ as the lake area changes (Equation (3)), $P_c(t)$ must further increase. However, from Equation (2), we note the volume of the descending magma is proportional to $Q_{mo}(t)$. This flow rate $Q_{mo}(t)$ is a function of $A_l(t)$, which varies according to the square of $h_l(t)$ (whose proportion factor depends on the inverted cone geometry, see Figure 2).

Consequently, the upward buoyancy force induced by the increase in the lava lake level is proportional to the square of $h_l(t)$ while the (downward) counter pressure (P_l) is linearly related to $h_l(t)$. This implies that the system of Equations (1) to (4) forms a positive loop gain. Without regulation, the outcome would be a lava lake filling unrealistically fast. In nature, fluid flow rates are inhibited by the physical parameters of the flow system (e.g., geometry of fluid flow conduits, fluid viscosities).

In general, the magmatic chambers that feed volcanoes have finite volumes. These volume restrictions imply that the mixing of resident magma with the intrusive degassed magma lessens the magma density contrast, which highly reduces the buoyancy force potential.

Additionally, the similar viscosity of the descending and ascending magma enhances mixing and further diminishes the buoyancy potential of ascending magmatic material [Huppert and Hallworth, 2007]. Taking into account these fluid effects, $P_c(t)$ can be expressed as,

$$P_c(t) = f(V_{in}) \frac{g\Delta\rho}{\pi d_a^2 / 4} \qquad (5)$$

where $g\Delta\rho$ represents the buoyancy force, and $f(V_{in})$ stands for the regulatory fluidic component of the system. This parameter can conveniently be modeled as a nonlinear function,

$$f(V_{in}) = \frac{b V_{in}}{(a + V_{in}^{1/n})^n} \qquad (6)$$

where *a* controls the slope of the function, and *b* and *n* control its amplitude and shape, respectively. Equation (6) exhibits a progression from a low initial flow that accelerates and approaches saturation over time. Through empirical bi-directional flow calculations, Huppert and Hallworth [2007] show that a higher mass flux occurs whenever either the viscosity ratio between descending and ascending fluid increases, or the conduit shortens (shown numerically as smaller *a* in Equation (6)). In order to ensure that $f(V_{in})$ does not provide a positive gain to the system (which is not considered physically realistic) the condition,

$$V_{in} / f(V_{in}) < 1 \qquad (7)$$

must be verified (which puts constraints on parameters *a*, *b*, and *n*). The observed temporal evolution of the lava lake level requires additional constraints on some of the model's physical parameters. For instance, if the conduit diameter (d_a) becomes too large or too small, either $\Delta\rho$ and/or α_{mo} must change according to the cumulate emplacement end-member model and may prove insufficient in supplying the required mass fluxes to maintain equilibrium.

5.1 Numerical Solutions

We consider two time periods, June 1982 - December 2001 and December 2002 - June 2011, for which field data on the lava lake evolution are available from time periods immediately following complete lava lake drainage; this is not the case for the period preceding the 1977 eruption for which the first documented lava lake level is -315 m in 1928 [Durieux, 2002/2003]. For both periods of time, and apart from the intrinsic crater morphology, the only parameter used to account for the different lava lake evolutions is $\Delta\rho$, which is varied within the range of 70 to 120 kg m^{-3}. Even though for each considered α_{mo} the value of $\Delta\rho$ must be adapted accordingly, this is clearly an advantage of having one main parameter whose tuning can account for a wide range of lava lake evolutions. Furthermore, because we consider a mixed entropy model, we calculate the solutions for α_{mo} to range from 1.3 x 10^{-5} (cumulate emplacement end-member model) to 7.5 x 10^{-5} (intrusive end-member model). For A_l = 46,550 m^2, this corresponds to Q_{mo} varying from 0.6 to 3.5 m^3 s^{-1}. Numerical solutions of Equations (1) to (6) corresponding to middle range α_{mo} are shown in Figure 8.

5.1.1 Period June 1982 to December 2001

During this ~20 year period, the lava lake level evolved through four main phases [SEAN, 1982; Tedesco 2002/2003]. Within a short period spanning ~3 months (June 26, 1982 to October 3, 1982) (phase 1), the lava lake level rose sharply before reaching a plateau, which lasted ~12 years (phase 2) (October 3, 1982 to June 22, 1994). During this quiescent period, a solid crust formed on top of the lava lake. A resurgence of activity started on June 22, 1994 and continued through December 1994 (phase 3) during which the intra-crateric magmatic activity was characterized by the presence of a wide (and extremely active) lava lake occupying the whole crater. This eruptive phase continued through August 1995. During this time, lava lake activity was related to a small spatter cone located inside the main crater, which allowed fresh magma to gently pour out onto a solid crust (P2) and expand across the main crater [Tedesco, 2002/2003].

Previous workers suggest that most of the crater floor was covered by a thin crust of freshly solidified lava, lying above a molten, partially or completely degassed body of magma [Tedesco, 2002/2003]. A progressive uplift of the crater floor between April and August of 1995 resulted from an accumulation of fresh magma at the base. In our model, this uplift corresponds to setting Q_{mo} = 0 and having $Q(t)$ set to a constant value in Equation (1). From August 1995 through December 2001 (phase 4), uplift and fresh magma flow ceased and the lava lake level stabilized at ~250 m below the crater rim (-250m).

For the periods when the lava lake was active (phases 1 and 3), we apply the default value range for α_{mo} (1.3 x 10^{-5} to 7.5 x 10^{-5}) (Table 4); otherwise during periods of quiescence corresponding to phases 2 and 4, we set α_{mo} to 2.0 x 10^{-9}, which corresponds to an average magma-supply rate of 3.0 kg s^{-1}, consistent with reported values of mass flux rates for those quiescent periods [Harris et al., 1999]. This quiescent mass flux rate is smaller than the volume flow rates necessary for keeping magma in a molten state, which allows for the formation of a solidified crust as reported by September, 1982 [Durieux, 2002/2003]. Finally, to fit the rise of the lava lake level during the resurgence of activity (phase 3), we have to decrease the initial value of $\Delta\rho$ by ~10%. This range assumes that (small) changes in magma properties occurred in the magmatic chamber.

One potential numerical solution of Equations (1) to (6) for the whole period (June 1982 to December 2001) is shown in Figure 8A. For phase 1, this simulation indicates that the lava lake volumes (measured at levels -500 m (at t =1 month) and -380 m (at t =2.6 months)) amount to 29 x 10^6 m^3 and 68 x 10^6 m^3, respectively. These values represent good

matches for Krafft's [SEAN, 1982] and Tazieff's [1984] estimates of 36 x 10^6 m^3 and 65 x 10^6 m^3, respectively, at correspondingly similar lava lake levels. These similarities provide reassurance for crater configuration consistent with the inverted cone model. Between June and December of 1994, ~24 x 10^6 m^3 of fresh magma was extruded, which is consistent with the volume reported (~25 x 10^6 m^3) for this period of time [GVN, 1995]. At the onset of phase 4 (December 2001), the numerical solution indicates that a total of 134 x 10^6 m^3 of magma had filled the crater, while 200 to 1400 x 10^6 m^3 of magma circulated back under the edifice. These values are comparable to the range of intruded volumes estimated during different time periods (e.g., 500 to 1700 x 10^6 m^3 estimated by Harris et al. [1999] for the period 1959 – 1972).

5.1.2 Period December 2002 to June 2011

For this period of time, the lava lake activity has been continuous without reported quiescent phases. The numerical solutions of Equations (1) to (6) for the whole time (Figure 8B) indicate that over this nine-year period, between 100 and 600 x 10^6 m^3 of magma must have cooled and circulated back under the edifice and 8.5 x 10^6 m^3 of molten lava filled the lava lake.

We further explored the possible evolution of the lava lake by numerically extrapolating to year 2022. By this time the lava lake surface might reach a level between −286 and −360 m with a volume ranging from 10 to 15 x 10^6 m^3, while between 300 to 1700 x 10^6 m^3 of magma could have been emplaced in the edifice or the crust beneath it. The simulation in Figure 8B shows the middle range for which the lava lake reaches a level of −339 m with a volume of 12 x 10^6 m^3 in the crater lake and 1100 x 10^6 m^3 of magma intruded/emplaced underneath Mt. Nyiragongo.

5.2 Lava Lake Instabilities

To account for the observed transient variations of the lava lake level (e.g., the ~25 m drop observed on June 3, 2011) or the slow metric fluctuations of the lava lake surface in June 2010, we consider the physical model developed by Witham and Llewellin [2006] for a generic lava lake system. According to their model, when the ratio of the cross-sectional areas of the conduit and lake is small (which is the case at Mt. Nyiragongo, i.e., $A_c / A_l = 3.8 \times 10^{-3}$ in June 2011), and the conduit contains a bubbly layer (ϕ in Figure 2), then the lake is most likely unstable, causing small fluctuations from the loss of bubbly

magma and/or more amplified drop-offs in reservoir pressure.

5.2.1 Drainage Events

Dissolved H_2O, which accounts for 0.5 to 0.8 wt% of Mt. Nyiragongo lavas (similar to other nephelinitic glasses; Dixon, 1997), is the most significant volatile component in the melt [Sawyer et al., 2008]. Based on these estimates for water content, we estimate that the volatile degassing of water at relatively low pressure (< 100 MPa in the conduit) could produce a small pressure reduction in the shallow magma reservoir. Lava lake drainage would stop only when the pressure at the base of the conduit equilibrates with the reservoir pressure. This equilibrium point is a function of the gas volume contained in the conduit and the volume displaced by the descending degassed magma. According to the chosen model parameters (Figure 2), the displacement of a bubbly gas layer would account for a pressure drop on the order of 0.5 MPa, and stabilization would occur at ~20 m below the initial level. Therefore, we suggest that a partial displacement of the gas volume can explain the pressure drop and account for the observed drop in the lava lake level. Such an explanation has previously been proposed to account for similar activity at other lava lake systems (e.g., Tilling 1987; Aster et al., 2003; Field et al., 2012; Spampinato et al., 2012). Gas displacement is a non-reversible process, and thus, in order to reach the initial (pre-perturbation) lava lake level, the reservoir pressure must increase beyond its initial value (Witham and Llewellin, 2006). Because of the aforementioned self-regulating magmatic system (Equations (1) to (6)), we predict that pressures will progressively build up and lava lake levels will increase.

5.2.2 Transient Rises of the Lava Lake Level

In June 2010, we observed transient fluctuations in the lava lake level on the scale of a few meters over three days. The scale of fluctuations was large enough to allow lava to flow over the rim (Figure 4B). Such a series of overflow events occurred at the end of each day (as reported in Table 1). Similar lava lake activities following diurnal patterns have previously been reported for Nyiragongo [Tazieff, 1975]. A two-meter rise of lava column, which requires a pressure increase of 52×10^3 Pa, can be explained by assuming an accumulated bubble layer in the upper conduit. The diurnal component of these fluctuations may result from negative barometric pressure variations (P_A in Figure 2). For example, many tropical areas experience diurnal (and semi-diurnal) barometric pressure oscillations on the order of 50-100 Pa [Dai and Wang, 1999; Ray, 2001] and may be one driver of this dynamic system.

To investigate this issue, we further utilize the model developed by Witham and Llewellin [2006] in order to estimate the amount of un-degassed magma required to significantly modify the gas volume fraction of the bubbly layer within the magmatic conduit. Small, negative pressure variations in the range of 50-100 Pa can augment the magma influx in the conduit by ~1-4%, with the effect of progressively (over 24 hours) modifying the gas volume fraction in the upper portion of the conduit. Because the bubbly layer introduces a nonlinear component, an increase of a few percent of its thickness (due to un-degassed ascending magma) can translate into a reduction of the column pressure by ~0.01 to 0.1 MPa, which in turn could lead to an increase of the lava lake level on a range of a few meters.

The numerical model clearly demonstrates that magmatic degassing conditions can affect the stability of the lava lake without invoking contributions from negative barometric pressure. Although atmospheric pressure may play a role in the diurnal lava lake fluctuations, it is not required. Thus, we conclude that the fluctuations likely remain dependent on undetermined degassing conditions.

6 Discussion and Conclusions

In this paper, we consider the short- and long-term dynamics of Mt. Nyiragongo's lava lake. The field data gathered since January 2002 suggest that the Mt. Nyiragongo volcano is slowly filling the volcanic edifice from a shallow magma chamber. While little is known about the subsurface structures of Mt. Nyiragongo, two main factors are relevant: (1) Mt. Nyiragongo's location in an extensional environment likely promotes a strong interaction with the magmatic body, erupting magma, and faulting [Corti et al., 2002/2003; Shuler and Ekström, 2009] and (2) there appear to be two intermittently connected magma reservoirs at different depths, which feed the magma. The shallow reservoir occurs at 1000 to 4000 m [Demant et al., 1994; Louaradi et al., 1993; Platz et al., 2004], while the deeper one is estimated to be at a depth of 10 to 14 km below the surface, as deduced from petrographic analysis [Demant et al., 1994; Platz et al., 2004], short-lived isotopes in lavas from the 2002 eruption [Chakrabarti et al., 2009], and seismic studies [Shuler and Ekström, 2009].

In an attempt to quantify the intrusive/extrusive volume ratio, we developed a simplified bi-directional flow model in which buoyancy force from (degassed) denser magma circulating back into the reservoir exerts a pressure sufficient to further push fresh magma into the lava lake. Numerical solutions of this self-regulating magmatic system indicate that the lava lake volume and intruded/emplaced magma volumes between January 1977 and December 2001 were 134 x 10^6 m^3 and 200 to 1400 x 10^6 m^3, respectively. These estimates

indicate that 10% to 67% of the total magma resides in the volcanic edifice. By comparison, the simulations indicate that between 2002 and 2011 only ~100 to 600 x 10^6 m^3 of magma was emplaced with ~ 300 to 1700 x 10^6 m^3 of additional emplacement by 2022. Because the lava lake volumes range from 8.5 x 10^6 m^3 in 2011 to possibly 15 x 10^6 m^3 by 2022 these calculations suggest that the magma being emplaced as dykes represents approximately 10 to 100 times the volume of magma contained in the lava lake. This magma volume range highlights an important outcome of our model and demonstrates the critical nature of the lava lake geometry in regulating the bi-directional magma flow (see Section 5).

The last two eruptive events offer a benchmark to calculate the part of the lava lake volume that may flow out of Mt. Nyiragongo during a future eruptive event. Other than the period between 1959-1972 when ~500 to 1700 x 10^6 m^3 of magma could have been emplaced below Mt. Nyiragongo [Harris et al., 1999], there are no reliable estimates of the ratio of emplaced magma volume for most of the last half-century of lava-lake activity (1928-1977). Approximately 22 x 10^6 m^3 of magma erupted from the lava lake during the January 1977 eruption, which represents about 10% of its total volume (~234 x 10^6 m^3) [Tazieff, 1977]. Similarly, the 2002 eruption (which consisted of ~26 x 10^6 m^3 of erupted lava [Komorowski et al., 2002/2003]) had minimal sourcing from the lava lake. Instead, Tedesco et al. [2007a] infer that while the smaller northern lava flows were probably supplied by the lava lake and shallow magma reservoir, the majority of the magmatic ejection occurred as part of the southern lava flows, and were sourced from a second, deeper and larger reservoir. This unrelated source is probably located beneath the city of Goma and Lake Kivu and encompasses a volume of ~136 x 10^6 m^3.

Wauthier et al. [2012] report that part of the January 2002 eruption was fed by a shallow dyke with a volume of ~74 x 10^6 m^3, most likely supplied through the lava lake drainage. Also, the lava flows erupting from vents 1 and 2 in the Shaheru area (Figure 2), which amount to ~2 x 10^6 m^3, most likely were directly supplied by the lava lake conduit system. For the lava flows spilling from the other vents located at lower altitude, about 6 x 10^6 m^3 and 15 x 10^6 m^3 were supposedly supplied by the shallow and deeper dyke, respectively. Thus, of the estimated 134 x 10^6 m^3 of magma that filled the crater in January 2002, only a portion of it (~55%) was apparently molten enough to drain into the shallow dyke, of which a small part (~10%) erupted. Of the rocky portion (~58 x 10^6 m^3), a minor part was expelled by the phreatomagmatic eruption, which followed the collapse of the inner parts of the crater [Komorowski et al., 2002/2003], but the largest part had to disappear into fractures, similar to the January 1977 crater collapse [Tazieff, 1977]. Assuming that activity

within the last decades is representative of the long-term historical activity of Nyiragongo, the small fraction (< 10%) of lava erupted throughout time implies an efficient convective circulation that remarkably preserves the lava lake and the shallow reservoir to a nearly constant volume.

One potential cause that may stimulate movement along the fragile and already widely fractured southern flank of Mt. Nyiragongo is the pressure that the lava within the crater creates on the internal crater walls; a pressure that is proportional to lava lake depth. Also, given the present crater configuration with a lava lake confined within a small part of the crater with a volume ten times smaller than before the January 2002 crater collapse, an eruptive event likely needs an external seismic/tectonic event (such as an earthquake) to trigger it.

It is important to note that even at the most conservative estimates of volumes of lava stored within the Mt. Nyiragongo volcano, there is a sufficient volume to pose a serious threat to the city of Goma and surrounding areas. The last eruption (January 2002) has shown that while only a small part of the lava lake erupted (less than 10%), a much larger amount of magma intruded into dykes, representing a significant volcanic hazard if a catastrophic fissural eruption similar to 2002 were to be repeated [Favalli et al., 2009; Wauthier et al., 2012]. Thus, even if the lava lake volume is predicted to range within 10 to 15 x 10^6 m^3 for the next decade, it does not reduce the risk of lava flows within the city of Goma. Indeed, if the shallow dyke is likely fed by the drainage of the lava lake, and consequently the amount of involved magma is bounded, the mechanism for feeding the deeper dyke is less clear. In our model, we assume that the convective magma (which could represent between 300 to 1700 x 10^6 m^3 by 2022) is in part emplaced within a magma chamber, while the other part is intruded into dykes. Wauthier et al. [2012] suggest that the deep, slowly filling dyke is either situated under the city of Goma or part of another slowly filling dyke system. They suggest the deep dyke they inferred might be too narrow to cause detectable InSAR displacements. However, it would be quite suitable to accommodate part of the cooler and denser convective magma, and thus represents a potential risk for future eruptions.

In conclusion, the threat of a future eruption, which is most likely to occur within the rift-related structures situated at the southern side of Mt. Nyiragongo, is even more significant in light of the high velocity silica-undersaturated lavas observed during the last two eruptions. Because the southern side of the volcanic edifice has a past history of eruptions and faces the largest urban population (in Goma), hazard monitoring should focus there first. Thus, we recommend continuous monitoring of the lava lake level by a

combination of satellite observations and direct field observations of lake level, fumarolic activity, and changes in the chemical composition of fumaroles and lava.

Acknowledgements

We gratefully acknowledge the European Union and Swiss Cooperation (DDC) for their continuous support to the UNOPS project "Analysis and Prevention of Natural Hazards in DRC". Our gratitude goes to Marc Caillet, Nathalie Duverlie, Olivier Grunewald, Patrick Marcel, Pierre Vetsch, and Ellen Campbell for their participation in the expedition's logistics, and to all the scientists from the Goma Volcano Observatory for their help and availability. We also thank Letizia Spampinato and an anonymous reviewer for their helpful comments, and Jean-Christophe Komorowski and Robert Poreda for their relevant comments on an earlier version of this manuscript.

Appendix A: Mathematical and Model Calculation Methods

Conduit Diameter

The maximum volume flow rate is determined by (1) the pressure (P_l in Figure 2) at the base of the lava lake (that is, ~13 MPa at this time for lake depth (h_l) of ~500 m) and (2) the fluid pressure in the flow direction, which depends on the conduit length (h_c). Large drainage volumes in short periods of time involving low magma viscosity (60 Pa·s for foiditic lavas [Giordano et al., 2007]) are characterized by a high Reynolds number ($R_e > 10^4$) and correspond to a turbulent flow regime. For a circular pipe in a turbulent regime, the volumetric flow rate can be determined using the Darcy–Weisbach equation [e.g., Bansal, 2010],

$$Q = \pi d_c^{5/2} \sqrt{\frac{P_l + \rho_d g h_c}{8 F h_c \rho_d}} \qquad (8)$$

where (Table 5) *g* is gravity acceleration, *F* is a friction factor which depends on the relative roughness of the conduit and the magnitude of the Reynolds number, d_c is the conduit diameter, h_c is the conduit length, the latter of which has a range estimated between 1000 to 4000 m [Demant et al., 1994; Louaradi et al., 1993; Platz et al., 2004], and ρ_d is density of

degassed magma, 2650 kg/m^3 for nephelinite [Carn, 2002/2003]. Setting $P_l = \rho_d g h_l$, the time needed to flush a magma volume V is

$$t = \frac{V}{\pi d_c^{5/2} \left(\frac{g}{8F}\right)^{1/2} \left(1 + \frac{h_l}{h_c}\right)^{1/2}} \qquad (9)$$

From this last equation it can be noted that conduit diameter rather than conduit length is the determinant factor when calculating the volumetric flow rate. To constrain the conduit diameter, we consider values of 7.5 m, 10 m, 12.5 m, and 15 m, which range within the reported values for basaltic volcanoes [Head and Wilson, 1987; Harris and Ripepe, 2007; Keating et al., 2008; Molina et al., 2012; Zandomeneghi et al., 2013]. Friction factor values are taken between 0.02 and 0.06 [Huppert and Sparks, 1985], which for the considered range of conduit diameters correspond (based on the Moody diagram, Moody, 1944) to mean heights of roughness of the pipe ε_c (Figure 2) from ~1 cm to ~50 cm. Figure 9 shows the calculated time lengths needed to flush 1.0 x 10^6 m^3 of magma for the considered ranges of conduit diameters and friction factors.

Effective Radiation Temperature and Energy Flux

Based on our 2010 and 2011 visual observation periods, we estimate that the average number of lava fountains that are simultaneously active is ~15, with base diameters in a range 5 to 15 m. Taking an average diameter of 10 m, we get f_{lava} = 2.5%. Based on photographs, we estimate the surface of the cracks represents about f_{crack} = 5% of the total surface, and we thus get f_{crust} = 92.5%, which allows us to calculate the effective radiation temperature,

$$T_e = (f_{lava} T_{lava}^4 + f_{crack} T_{crack}^4 + f_{crust} T_{crust}^4)^{0.25} \quad (10)$$

where T_{lava} = 1380 K [Sawyer et al., 2008], T_{crack} = 1150 K and T_{crust} = 750 K [Spampinato et al., 2013]. With these values we get the effective radiation temperature T_e = 828 K.

Assuming the emission of radiation by the gas plume is negligible [Sawyer et al., 2008], heat loss is mainly driven by both radiative and convective cooling [Harris et al., 1999]. The radiative heat flux component is provided by,

$$\Phi_r = \sigma \varepsilon A_l T_e^4 \qquad (11)$$

with the Stefan-Boltzmann constant σ=5.668 x 10^{-8} W m^{-2} K^{-4}, T_e the effective radiation

temperature (828 K), ε the emissivity (set to 0.9, a conservative value, Burgi et al., 2002), and A_l the lava lake area (46,550 m^2). With these values, we get Φ_r = 1.1 GW.

For the convective cooling, we apply the equation describing the natural convection for heated horizontal surfaces facing upwards in the turbulent range [McAdams, 1959],

$$\Phi_{conv} = A_l h_{\Delta T} \Delta T \qquad (12)$$

where $\Delta T = T_e - T_{air}$, with T_{air} the average ambient air temperature (288.5 K), and $h_{\Delta T}$ =14 W m^{-2} K^{-1} the heat transfer coefficient of the air.

Mass Flux

The mass flux (*q*) required to yield an amount of heat loss Φ_{tot} (1.5 GW) can be calculated using (see for instance in Francis et al., 1993),

$$q = \frac{\Phi_{tot}}{C_L \Delta f + c_p \Delta T_{magma}} \qquad (13)$$

in which C_L is latent heat of crystallization (4.2 x 10^5 J kg^{-1}), c_p is the specific heat capacity of the magma (1150 J kg^{-1} K^{-1}), Δf the crystallized magma mass fraction, and ΔT_{magma} the temperature interval over which the magma cools.

References

Aster R, Mah S, Kyle P, McIntosh W, Dunbar N, Johnson J, Ruiz M, McNamara S (2003) Very long period oscillations of Mount Erebus Volcano. J Geophys Res 108. doi:10.1029/2002JB002101

Bansal RK (2010) A Textbook of Fluid Mechanics. Firewall Media

Baxter P, Allard P, Halbwachs M, Komorowski J-C, Woods A, Ancia A (2002/2003) Human health and vulnerability in the Nyiragongo Volcano eruption and humanitarian crisis at Goma, Democratic Republic of Congo. Acta Vulcanologica, Istituti Editoriali e Poligrafici Internazionali, Pisa – Roma, Vol. 14 (1-2), 2002 and Vol. 15 (1-2) 2003, 109-114

Bouche E, Vergniolle S, Staudacher T, Nercessian A, Delmonta J.-C , Frogneux M, Cartault F, Le Pichond A (2010) The role of large bubbles detected from acoustic measurements on the dynamics of Erta 'Ale lava lake (Ethiopia). Earth Planetary Sci Lett 295 : 37–48

Burgi P-Y, Caillet M, Haefeli S (2002) Field temperature measurements at Erta'Ale Lava Lake, Ethiopia. Bull Volcanol 64: 472–485

Calkins J, Oppenheimer C, Kyle PR (2008) Ground-based thermal imaging of lava lakes at Erebus volcano, Antarctica. J Volcanol Geotherm Res 177: 695–704

Carn SA (2002/2003) Eruptive and passive degassing of sulphur dioxide at Nyiragongo volcano (D. R. Congo): The 17th January 2002 eruption and its aftermath. Acta Vulcanologica, Istituti Editoriali e Poligrafici Internazionali, Pisa – Roma, Vol. 14 (1-2), 2002 and Vol. 15 (1-2) 2003, 75–85

Chakrabarti R, Basu, AR, Santo AP, Tedesco D, Vaselli O (2009) Isotopic and geochemical evidence for a heterogeneous mantle plume origin of the Virunga volcanics, Western rift, East African Rift system. Chemical Geology 259: 273-289

Corti G, Bonini M, Innocenti F, Manetti P, Mulugeta G, Sokoutis D, Cloetingh (2002/2003) Rift-parallel magma migration and localisation of magmatic activity in transfer zones. Acta Vulcanologica, Istituti Editoriali e Poligrafici Internazionali, Pisa – Roma, Vol. 14 (1-2), 2002 and Vol. 15 (1-2) 2003, 17-25.

Cuoco E, Tedesco D, Poreda RJ, Williams JC, De Francesco S, Balagizi C, Darrah TH (2013) Impact of volcanic plume emissions on rain water chemistry during the January 2010 Nyamuragira eruptive event: Implications for essential potable water resources. J Hazardous Materials 244:570-581

Dai A, Wang J (1999) Diurnal and Semidiurnal Tides in Global Surface Pressure Fields. J Atmospheric Sci 56 : 3874- 3891

Demant A, Lestrade P, Lubala RT, Kampunzu AB, Durieux J (1994) Volcanological and petrological evolution of Nyiragongo volcano, Virunga volcanic field, Zaire. Bull Volcanol 56: 47-61

Dixon JE (1997) Degassing of alkalic basalts. Am Mineral 82: 368–378

d'Oreye N, Fernandez J, Gonzalez P, Kervyn F, Wauthier C, Frischknecht C, Calais E, Heleno S, Cayol V, Oyen A, Marinkovic P (2008) Systematic InSAR monitoring of African active volcanic zones: What we have learned in three years, or an harvest beyond our expectations. In: Use of Remote Sensing Techniques for Monitoring Volcanoes and Seismogenic Areas. doi: 10.1109/USEREST.2008.4740361

d'Oreye N, Gonzalez PJ, Shuler A, Oth A, Bagalwa L, Ekstrom G, Kavotha D, Kervyn F, Lucas C, Lukaya F, Osodundu E, Wauthier C, Fernandez J (2011) Source parameters of the 2008 Bukavu-Cyangugu earthquake estimated from InSAR and teleseismic data. Geophys J Int 184: 934–994

Durieux J (2002/2003) Volcano Nyiragongo (D.R.Congo): Evolution of the crater and lava lakes from the discovery to the present. Acta Vulcanologica, Istituti Editoriali e Poligrafici Internazionali, Pisa – Roma, Vol. 14 (1-2), 2002 and Vol. 15 (1-2) 2003, 137-144

Durieux J (2008) Rapport de mission de terrain au volcan Nyiragongo. UNOPS.

Ebinger C (2005) Continental break-up: The East African perspective. Astronomy Geophys 46: 16-21

Favalli M, Chirico GD, Papale P, Pareschi MT, Boschi E (2009) Lava flow hazard at Nyiragongo volcano, D.R.C. Bull Volcanol 71: 363-374

Field L, Barnie T, Blundy , Brooker RA, Keir D, Lewi E, Saunders K (2012) Integrated field, satellite and petrological observations of the November 2010 eruption of Erta Ale. Bull Volcanol 74:2251-2271

Francis P, Oppenheimer C, Stevenson D (1993) Endogenous growth of persistently active

volcanoes. Nature 366: 554-557

Giordano D, Polacci M, Longo A, Papale P, Dingwell DB, Boschi E, Kasereka M (2007) Thermo-rheological magma control on the impact of highly fluid lava flows at Mt. Nyiragongo. Geophys Res Lett 34. doi: 10.1029/2006GL028459

GVN (1995) Bull Global Volcanism Net 20(1)

GVN (2001) Bull Global Volcanism Net 26(3)

GVN (2003) Bull Global Volcanism Net 28(2,5)

GVN (2006) Bull Global Volcanism Net 31(3)

Harris AJL, Flynn LP, Rothery DA, Oppenheimer C, Sherman SB (1999) Mass flux measurements at active lava lakes: Implications for magma recycling. J Geophys Res 104: 7117-7136

Harris A, Ripepe M (2007) Synergy of multiple geophysical approaches to unravel explosive eruption conduit and source dynamics – A case study from Stromboli. Chemie der Erde 67: 1–35

Head JW, Wilson L (1987) Lava fountain heights at Pu'u 'O'o, Kilauea, Hawaii: Indicators of amount and variations of exsolved magma volatiles. J Geophys Res 92: 2156-2202

Huppert HE, Sparks RSJ (1985) Cooling and contamination of mafic and ultramafic magmas during ascent through continental crust. Earth Planetary Sci Lett 74:371-386

Huppert HE, Hallworth MA (2007). Bi-directional flows in constrained systems. J Fluid Mechanics, 578: 95-112. doi:10.1017/S0022112007004661

Keating GN, Valentine GA, Krier DJ, Perry FV (2008) Shallow plumbing systems for small-volume basaltic volcanoes. Bull Volcanol 70:563-582

Komorowski J-C, Tedesco D, Kasereka M et al (2002/2003) The January 2002 flank eruption of Nyiragongo volcano (Democratic Republic of Congo) : Chronology, evidence for a tectonic trigger, and impact of lava flows on the city of Goma. Acta Vulcanologica, Istituti Editoriali e Poligrafici Internazionali, Pisa – Roma, Vol. 14 (1-2), 2002 and Vol. 15 (1-2) 2003, 27-61

Le Guern F (1987) Mechanism of energy transfer in the lava lake of Niragongo (Zaire), 1959-1977. J Volcanol Geotherm Res 31: 17-31

Louaradi D, Clochiatti R, Pineau F, Javoy M (1993) Magma storage beneath Nyiragongo volcano (Zaire): evidence from fluid and melt inclusions. Terra Abstracts 5:573

McAdams WH (1959) Heat transmission. McGraw-Hill, New York

Molina I, Burgisser A, Oppenheimer C (2012) Numerical simulations of convection in crystal-bearing magmas: A case study of the magmatic system at Erebus, Antarctica. J Geophys Res, B07209, doi:10.1029/2011JB008760

Moody LF (1944) Friction factors for pipe flow. Trans. ASME 66:671-678

Nyblade AA, Owens TJ, Gurrola H, Ritsema J, Langston CA (2000) Seismic evidence for a deep upper mantle thermal anomaly beneath east Africa. Geology 28: 599-602

Oppenheimer C, Lomakina AS, Kyle PR, Kingsbury NG, Boichu M (2009) Pulsatory magma supply to a phonolite lava lake. Earth and Planetary Sci Lett 284: 392–398

Platz T, Foleyb SF, André L (2004) Low-pressure fractionation of the Nyiragongo volcanic

rocks, Virunga Province, D.R. Congo. J Volcanol Geotherm Res 136: 269– 295

Poland M (2006) InSAR captures rifting and volcanism in East Africa. Alaska Satell. Facil. News Notes 3:1-3

Ray RD (2001) Comparisons of global analyses and station observations of the S_2 barometric tide. J Atmosph Solar-Terrestrial Physics 63: 1085–1097

Sawyer GM, Carn SA, Tsanev VI, Oppenheimer C, Burton M (2008) Investigation into magma degassing at Nyiragongo volcano, Democratic Republic of the Congo. Geochem Geophys Geosyst. doi :10.1029/2007GC001829

SEAN (1982) Bull Sci Event Alert Net Vol. 7(7, 10). Smithonian National Museum of Natural History. Washington DC (USA)

Sebai A, Stutzmann E, Montagner JP, Sicilia D, Beucler E (2006) Anisotropic structure of the African upper mantle from Rayleigh and Love wave tomography. Physics Earth Planetary Interiors 155: 48-62

Shuler A, Ekström G (2009) Anomalous earthquakes associated with Nyiragongo volcano: Observations and potential mechanisms. J Volcanol Geotherm Res 181: 219– 230

Smets B, d'Oreye N, Kervyn F, Kervyn M, Albino F, Arellano SR, Bagalwa M, C Balagizi, Carn SA, Darrah TH, Fernández J, Galle B, González PJ, Head E, Karume K, Kavotha D, Lukaya F, Mashagiro N, Mavonga G, Norman P, Osodundu E, Pallero JLG, Prieto JF, Samsonov S, Syauswa M, Tedesco D, Tiampo K, Wauthier C, Yalire MM (2014) Detailed multidisciplinary monitoring reveals pre-and co-eruptive signals at Nyamulagira volcano (North Kivu, Democratic Republic of Congo). Bull Volcanology 76:1-35

Smithsonian Institution/USGS Weekly Report (2011-2013) New Activity/Unrest: Nyiragongo, 16 November-22 November 2011; 31 October-6 November 2012; 31 July-6 August 2013. http://volcano.si.edu/reports_weekly.cfm

Spampinato L, Oppenheimer C, Cannata A, Montalto P, Salerno GG, Calvari S (2012) Bull Volcanol 74:1281-1292

Spampinato L, Ganci G, Hernández PA, Calvo D, Tedesco D, Pérez NM, Calvari S, Del Negro C, Yalire MM (2013) Thermal insights into the dynamics of Nyiragongo lava lake from ground and satellite measurements. J Geophys Res 118: 1-14

Stevenson DS, Blake S (1998) Modelling the dynamics and thermodynamics of volcanic degassing. Bull Volcanol 60: 307–317

Tassi F, Vaselli O, Tedesco D, Montegrossi G, Darrah T, Cuoco E, Mapendano MY, Poreda R, Delgado Huertas A (2009). Water and gas chemistry at Lake Kivu (DRC): Geochemical evidence of vertical and horizontal heterogeneities in a multi-basin structure. Geochem Geophys Geosyst 10. doi:10.1029/2008GC002191.

Tazieff H (1975) Niragongo ou le volcan interdit. Flammarion, Paris.

Tazieff H (1977) An exceptional eruption: Mt Nyiragongo, Jan 10th 1977. Bull Volcanol 30: 189– 200

Tazieff H (1984) Mt. Nyiragongo: renewed activity of the lava lake. J Volcanol Geotherm Res 20: 267– 280

Tazieff H (1994) Permanent lava lakes: observed facts and induced mechanisms. J Volcanol Geotherm Res 63: 3-11

Tedesco D (2002/2003) 1995 Nyiragongo and Nyamulagira activity in the Virunga National

Park: A volcanic crisis. Acta Vulcanologica, Istituti Editoriali e Poligrafici Internazionali, Pisa – Roma, Vol. 14 (1-2), 2002 and Vol. 15 (1-2) 2003, 149-155

Tedesco D, Vaselli O, Papale P, Carn SA, Voltaggio M, Sawyer GM, Durieux J, Kasereka M, Tassi F (2007a) January 2002 volcano-tectonic eruption of Nyiragongo volcano, Democratic Republic of Congo. J Geophys Res. doi: 10.1029/2006JB004762

Tedesco D, Badiali L, Boschi E, Papale P, Tassi F, Vaselli O, Kasereka C, Durieux J, DeNatale G, Amato A, Cattaneo M, Ciraba H, Chirico GD, Delladio A, Demartin M, Favalli G, Franceschi D, Lauciani V, Mavonga G, Monachesi G, Pagliuca NM, Sorrentino D, Yalire M (2007b) Cooperation on Congo volcanic and environmental risks Eos Trans AGU 88:177-181. doi: 10.1029/2007EO160001

Tedesco D, Tassi F, Vaselli O, Poreda RJ, Darrah T, Cuoco E, Yalire MM (2010) Gas isotopic signatures (He, C, and Ar) in the Lake Kivu region (western branch of the East African rift system): Geodynamic and volcanological implications. J Geophys Res. doi: 10.1029/2008JB006227

Tilling RI (1987) Fluctuations in surface height of active lava lakes during 1972-1974 Mauna Ulueruption, Kilauea volcano, Hawaii. J Geophys Res 92: 13721-13730

Wauthier C, Cayol V, Kervyn F, d'Oreye N (2012) Magma sources involved in the 2002 Nyiragongo eruption, as inferred from an InSAR analysis. J Geophys Res. doi: 10.1029/2011JB008257

White R, McKenzie D (1989) Magmatism at rift zones. The generation of volcanic continental margins and flood basalts. J Geophys Res 94: 7685-7729

Witham F, Llewellin EW (2006) Stability of lava lakes. J Volcanol Geotherm Res 158: 321–332

Witter JB, Kress VC, Delmelle P, Stix J (2004) Volatile degassing, petrology, and magma dynamics of the Villarrica Lava Lake, Southern Chile. J Volcanol Geotherm Res 134: 303– 337

Wright R, Pilger E (2008) Radiant flux from Earth's subaerially erupting volcanoes. Int J Remote Sensing 29: 6443–6466

Zandomeneghi D, Aster R, Kyle P, Barclay A, Chaput J, Knox H (2013) Internal structure of Erebus volcano, Antarctica imaged by high-resolution active-source seismic tomography and coda interferometry. J Geophys Res 118: 1067–1078

Table 1: Occurrence Time and Magnitude of Lava Overflows

Day (2010)	Time (GMT+2)	Amplitude of the overflows
June 19th	14:30; 14:56; 15:38	Small
	15:57	Large
	17:29	Large
June 20th	17:09; 17:20	Small
	17:50; 18:10	Large
	19:07	Small
	19:20	Large
June 21st	15:46; 16:31	Small
	19:29	Large

Table 2: Lava lake level[1] and diameter from January 1977 to January 2002

Date	Lava lake level (m)	Lava lake diameter (m)	References
January 13th, 1977	-800	-	Durieux [2002/2003]
June 26th, 1982	-730	250	SEAN [1982]
June 27th, 1982	-630	309	Tazieff [1984]
June 30th, 1982	-680	300	SEAN [1982]
July 7th, 1982	-555	N/A[2]	Durieux [2002/2003]
Early July, 1982	-530	436	Tazieff [1984]
July 23nd, 1982	-500	600	SEAN [1982]
August 4th, 1982	-380	727	Tazieff [1984]
October 3nd, 1982	-340	818	Tazieff [1984]
June 23nd, 1994	-340	N/A	Durieux [2002/2003]
August 20th, 1994	-310	N/A	Durieux [2002/2003]
December 10th, 1994	-295	800	Durieux [2002/2003]; GVN [1995]
August 1995-January 17th, 2002	-250	900	Durieux [2002/2003]; GVN [2001]

[1] The 3,425 m SE rim is taken as reference

[2] N/A: Not Available

Table 3: Lava lake level[1] and diameter from January 2002 to June 2011

Date	Lava lake level (m)	Lava lake Diameter (m)	References
January 24th, 2002	-900	-	Tedesco et al. [2007a]
December 18th, 2002	-830	50	GVN [2003]
January, 2003	-800	100	GVN [2003]
August, 2003	-700	N/A[2]	Durieux [2008]
January, 2006	-540	200	GVN [2006]; Sawyer et al. [2008]
May, 2006	-531	N/A	Durieux [2008]
July, 2007	-476	N/A	Durieux [2008]
March, 2008	-400	N/A	Durieux [2008]
June, 2010	-385	225	Present study
June 2nd, 2011	-415	240	Present study
June 8th, 2011	-445	~240	Present study

[1] The 3,425 m SE rim is taken as reference

[2] N/A: Not Available

Table 4: Parameters for Mass Flux Calculations

	High End Member	Low End Member	
Δf	0.25	1	
ΔT_{magma}	50 °C	400 °C	
q	9230 kg s^{-1}	1704 kg s^{-1}	
	(0.2 kg $s^{-1}m^{-2}$)		
Q_{mo}	3.48 m^3 s^{-1}	0.64 m^3 s^{-1}	Range: 0.6 – 3.5 m^3 s^{-1}
α_{mo}	7.5 x 10^{-5} m^3 s^{-1} m^{-2}	1.3 x 10^{-5} m^3 s^{-1} m^{-2}	

Table 5: Description of Symbols and Subscripts Used

Symbol	Property	Value, Unit
$\rho\square$	Density of degassed magma	kg m^{-3}
$\Delta\rho$	Magma density contrast	kg m^{-3}
F	Friction factor	
R_e	Reynolds number	
g	Gravity acceleration	9.81 m s^{-2}
ε_c	Mean height of roughness	m
Δf	Crystallized magma mass fraction	
ΔT_{magma}	Temperature interval over which the magma cools	°C
f	Fraction area	
T	Temperature	K
T_{air}	Average ambient air temperature	K
$h_{\Delta T}$	heat transfer coefficient of air	W $m^{-2}K^{-1}$
μ	Magma viscosity	Pa s
c_p	Magma's specific heat capacity	J kg^{-1} K^{-1}
C_L	Latent heat of crystallization	J kg^{-1}
σ	Stefan-Boltzmann constant	W $m^{-2}K^{-4}$
ε	Emissivity	
Φ_r	Radiative heat flux	W
Φ_{conv}	Convective heat flux	W
Φ_{tot}	Total heat loss	W
P	Pressure	Pa
P_A	Atmospheric pressure	Pa
h	Height	m
d	Diameter	m
d_0	Diameter of the base of the inverted cone	m
A	Area	m^2
V	Volume	m^3
T_e	Effective radiation temperature	K
q	Mass flux	kg s^{-1}
Q	Volume flow rate	m^3 s^{-1}
Q_{mo}	Minimum volume flow rate to keep lava in molten state	m^3 s^{-1}
α_{mo}	Q_{mo} per m^2	m^3 s^{-1} m^{-2}
γ	Repose angle	deg
Subscripts		
a	Ascent (ρ, d)	
b	Bubbly layer (h, P)	
c	Conduit (A, d, h, P)	
in	Intruded (V)	
l	Lake (A, d, V, h, P)	
r	Reservoir (P)	
crack	Glowing central core surrounded by cooler crust (f, T)	
crust	(f, T)	
lava	(f, T)	

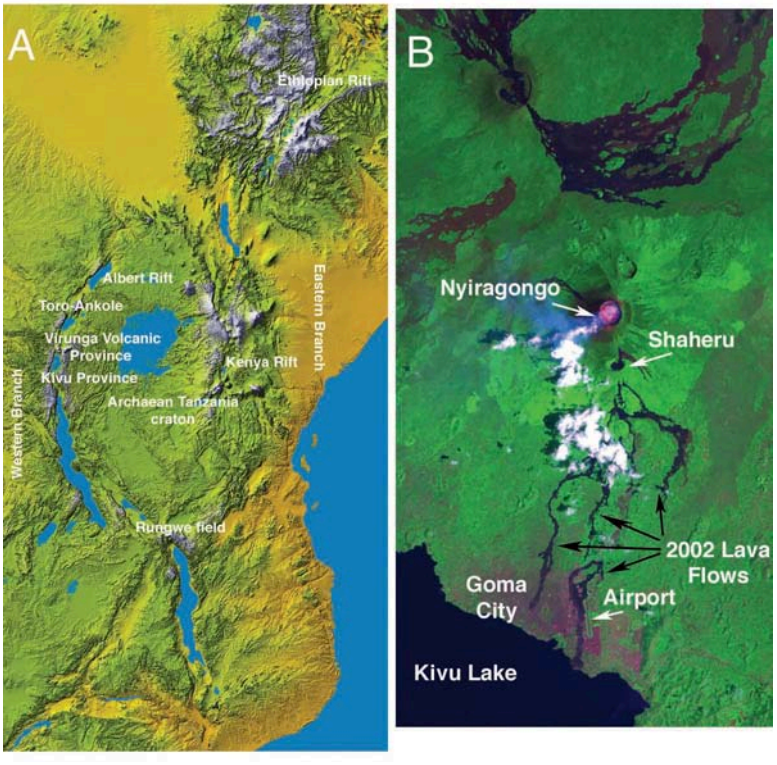

Figure 1. Mt. Nyiragongo within the Western branch of the EARS. A. Space Shuttle radar topography image with the main landmarks of the Western branch of the East African Rift highlighted. B. Landsat 7 satellite image of the Virunga volcanic province, captured on January 31, 2003, on which Nyiragongo lava fields from the 2002 eruption are indicated with black arrows. Mt. Nyiragongo's summit is located 18 km north of Goma city. Images, courtesy of NASA.

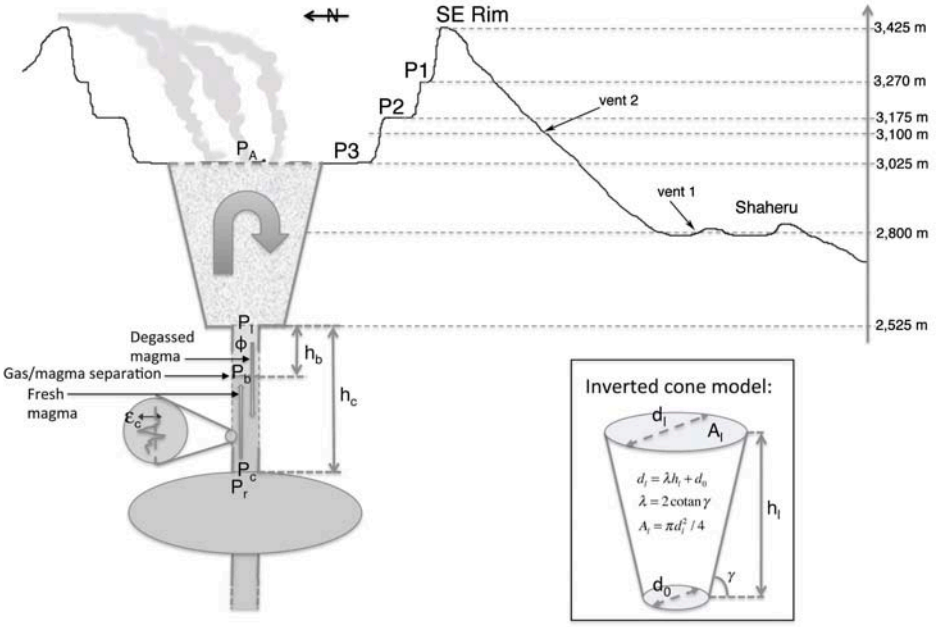

Figure 2. Topography of Mt. Nyiragongo's volcanic crater and conduit model. Schematic representation of the lava lake with reference to the January-2002 erupting vents 1 and 2 [cf., Komorowski et al., 2002/2003]. The total declination from the SE rim (altitude 3,425 m, usual reference) to the crater floor (P3) is ~400 m, with P2 and P1 corresponding respectively to the 2002 and 1977 lava lake levels. The shallow reservoir (h_c in range 1000 to 4000 m) is connected to the lava lake through a vertical conduit (of diameter d_c with mean height roughness ε_c), open to the atmosphere with P_A = ~0.071 MPa. Conduit and reservoir pressures are indicated by P_c and P_r, respectively. Conduit model: Below a critical pressure (P_b), exsolution becomes significant and produces a bubble suspension in part ϕ of the conduit. Assuming the H_2O mass fraction is 0.8 wt%, and setting P_b to 20 MPa, then h_b = 309 m. Inset: The inverted cone model.

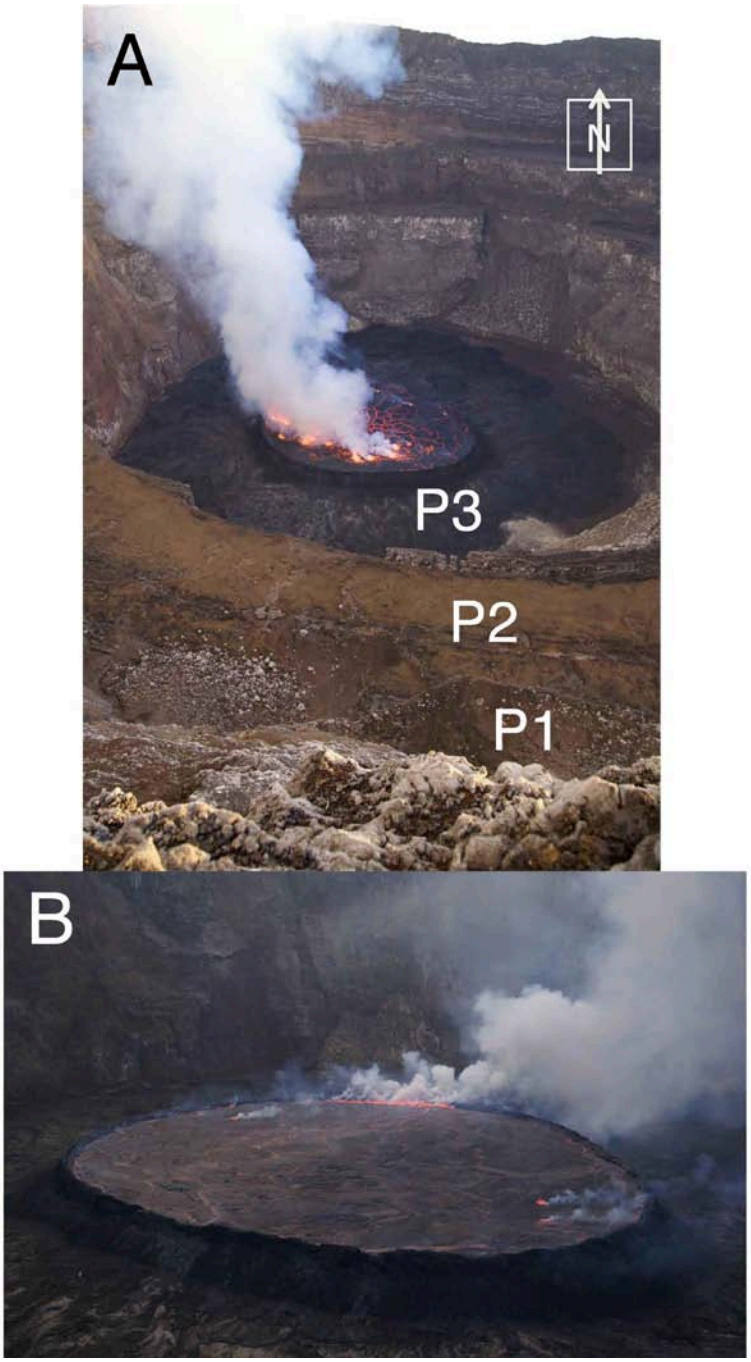

Figure 3. General view of Mt. Nyiragongo's volcanic crater. A. View of the three platforms (P1, P2, and P3) taken from the SE rim along the N-S direction. Typical lava lake activity with lava fountains and glowing cracks surrounded by cooler crust (photo taken on June 15th, 2010). B. Lava lake configuration, about 15 m higher than P3, with magma close to top of the levee (photo taken on June 19th, 2010).

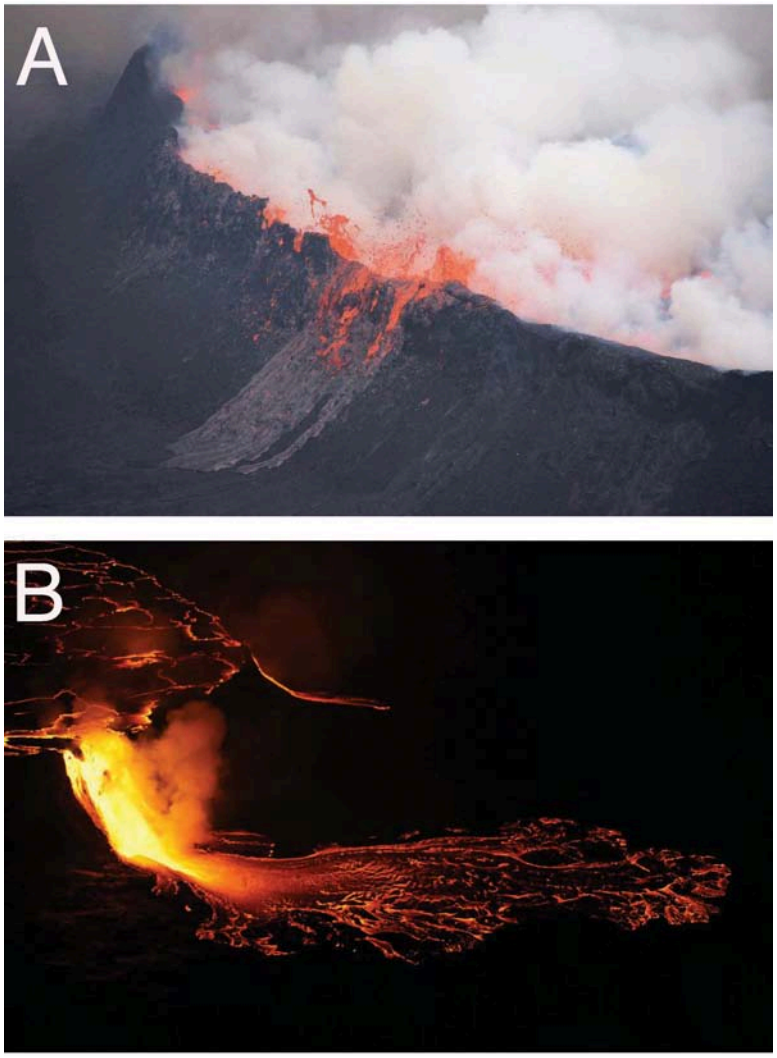

Figure 4. Levee overflows. A. Small overflow on the south side of the levee due to a lava fountain colliding against the levee cliff (photo taken on June 21st, 2010, at 3:15 pm). B. Large overflow on the SE side (photo taken on June 20th, 2010, at 6:50 pm).

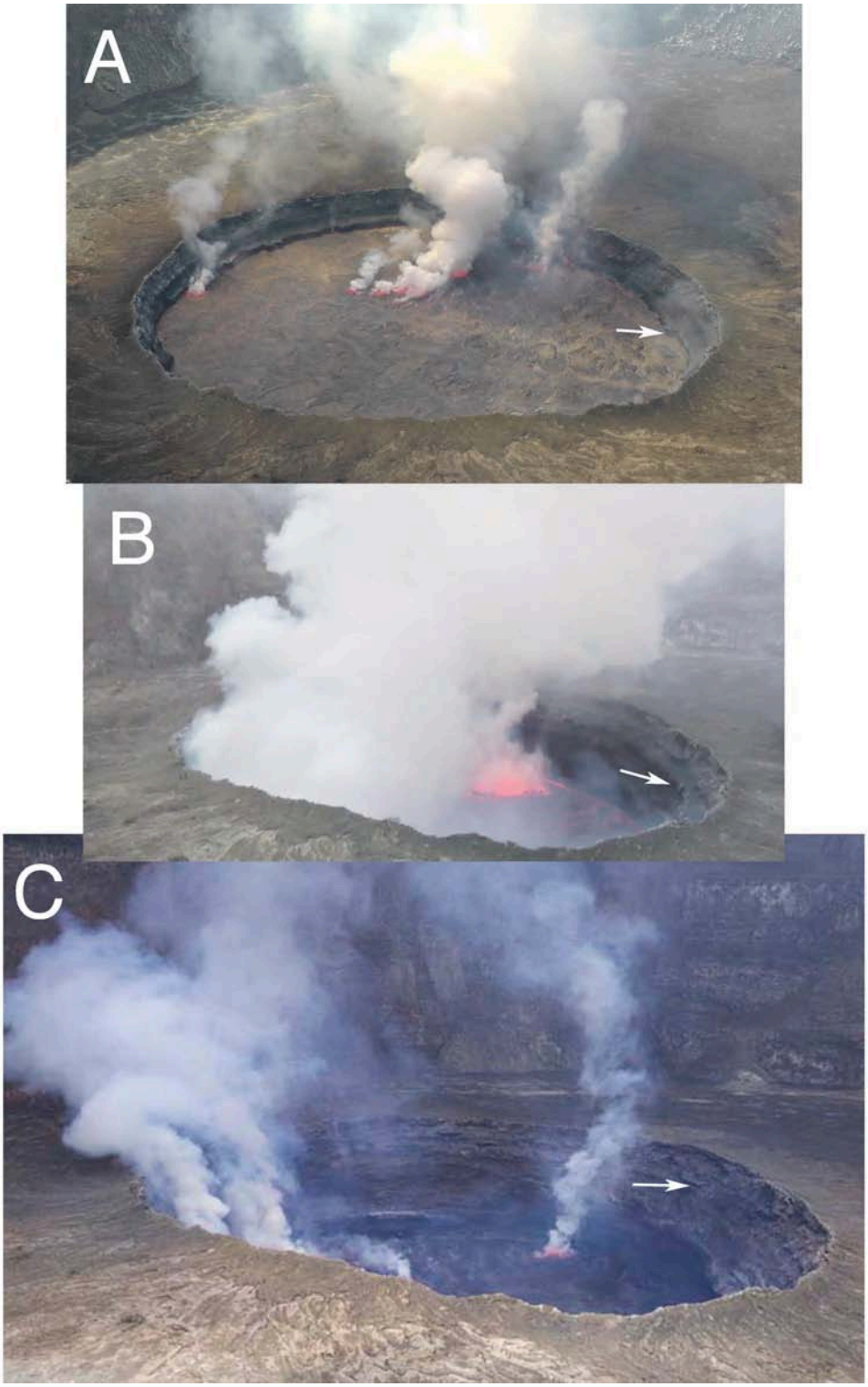

Figure 5. Lava lake level from the levee in 2011. (A) -12 m, June 2nd (2:00 pm); (B) -37 m, June 4th (8:15 am); (C) -45 m, June 8th (9:45 am). White arrows in the 3 panels indicate the -12 m lava lake level. Photos courtesy of Patrick Marcel.

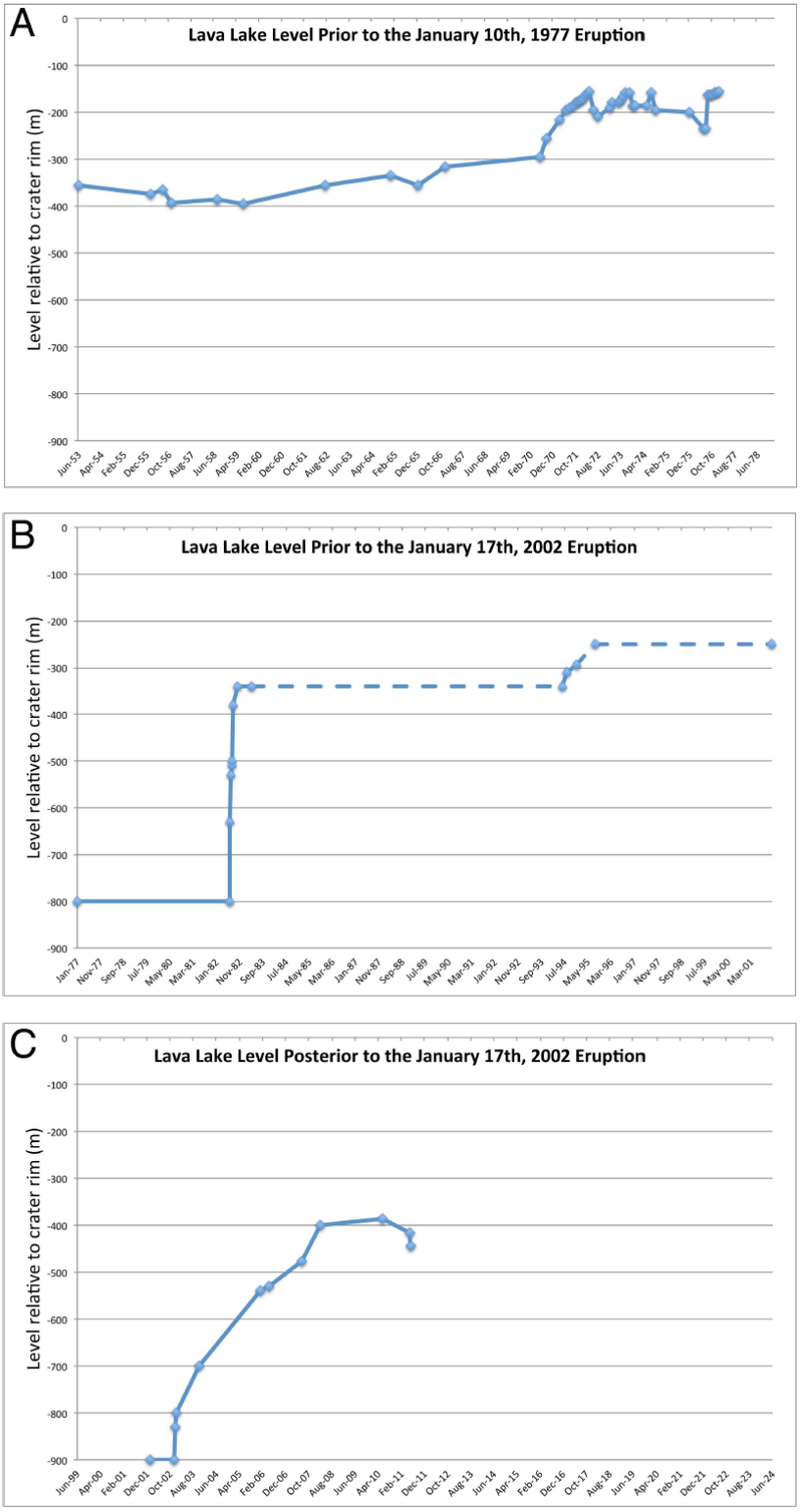

Figure 6. Evolution of the lava lake level. A: June 1953 to January 1977 [Durieux, 2002/2003] B: January 1977 to December 2001 (Table 2); inactive periods between early 1983 and June 1994, and September 1995 to December 2001 are indicated with dashed lines. C: January 2002 to June 2011 (Table 3). The 3,425 m SE rim is taken as reference.

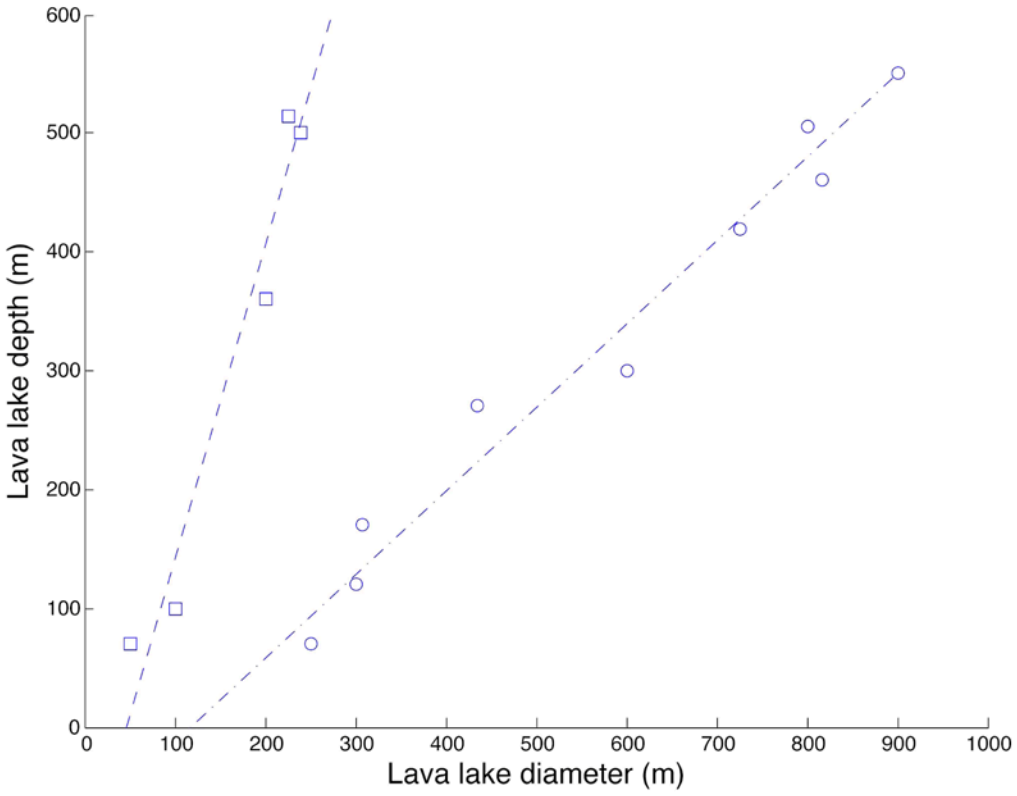

Figure 7. Correlation between lava lake diameter (d_l) and lava lake depth (h_l). Circles and squares are field data corresponding respectively to the June 1982 - December 2001 (Table 2) and December 2002 - June 2011 (Table 3) periods. Linear regression (dashed lines) correspond to the inverted cone model (cf., Figure 2) with λ=1.42 and d_0=118 m (for circles) and λ=0.38 and d_0=46 m (for squares).

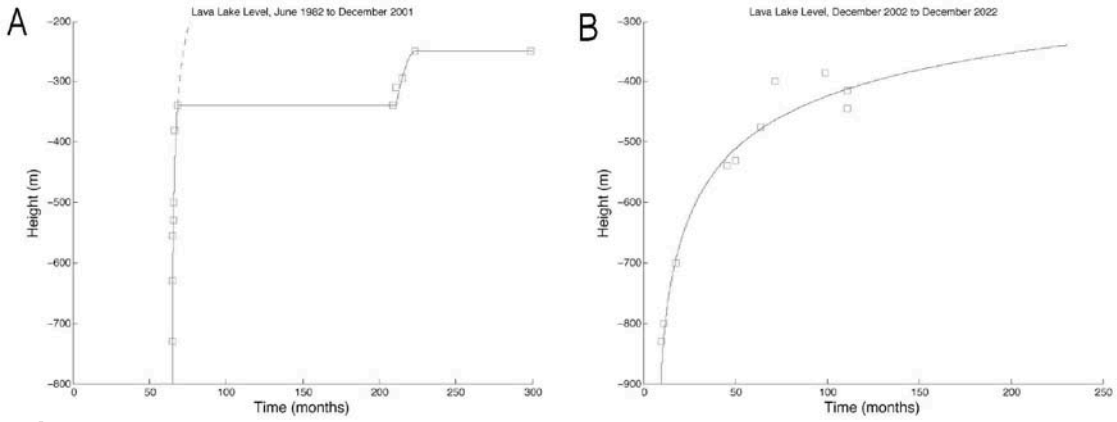

Figure 8. Model for the evolution of the lava lake level. The small squares stand for the field measurements (visible also in Figure 6), and the solid curves are the fits obtained by numerical resolution of Equations (1) to (6). A. From June 1982 to December 2001. The model takes into account the quiescence periods between mid-September 1982 and June 1994, and August 1995 to December 2001 during which the mass flux rate has been set to ~3 kg s^{-1}. The dashed line shows the progression of the lava lake level if the quiescent period did not occur. From June 24th, 1982 to June 1994, $\Delta\rho$ = 88 kg m^{-3}; for the resurgence period from June 1994 to August 1995, $\Delta\rho$ = 79 kg m^{-3}; between April 1995 and August 1995, Q_{mo} = 0 and $Q(t)$ set to 0.8 m^3 s^{-1} B. Simulation from December 2002 to June December 2022 with parameter $\Delta\rho$ = 79 kg m^{-3}. For all simulations α_{mo} = 4.9 x 10^{-5} m^3 s^{-1} m^{-2} (which corresponds to Q_{mo} = 2.3 m^3 s^{-1} for A_l = 46,550 m^2); n=4; a = 24 $m^{1/4}$; b = 1.9 x 10^6 m^3; d_a = 9.0 m; h_c = 4000 m; μ=60 Pa s; time step 60 s.

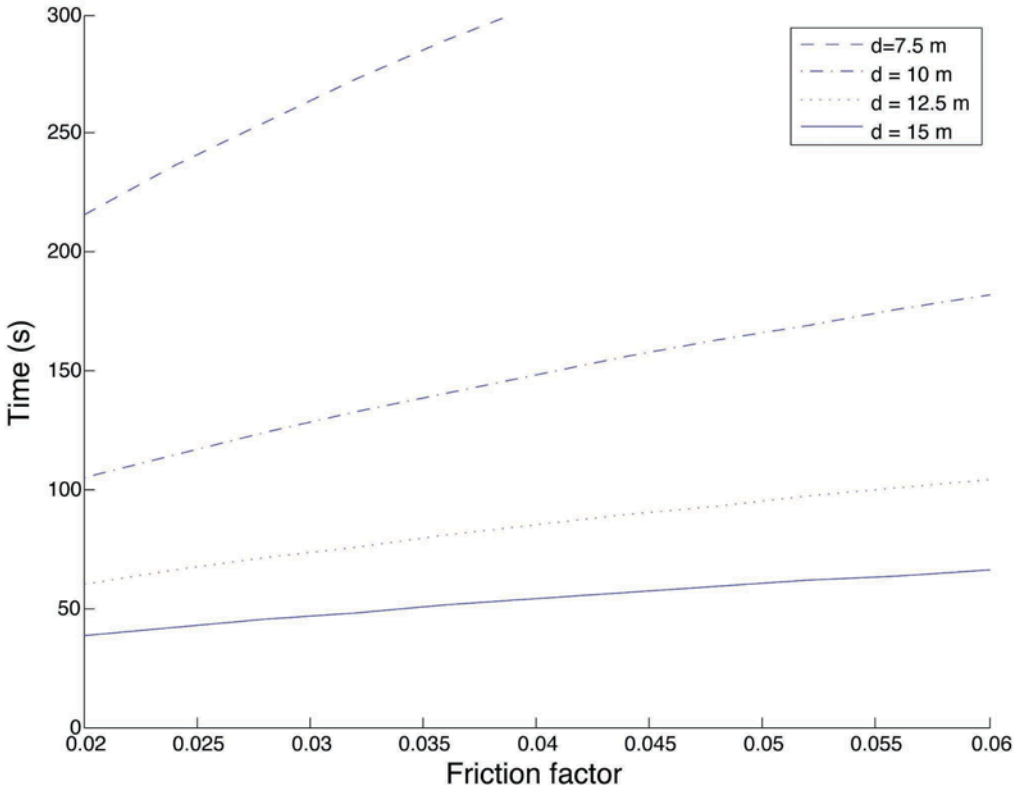

Figure 9. Time needed for flushing about one million cubic meter of magma as a function of friction factor (F) for a range of conduit diameters (Equation (9)). Lave lake depth h_l = 500 m and conduit length h_c = 1000 m; for a conduit length of 4000 m, time increases by about 10%.